

Research Article

Characteristics and Gas-Bearing Properties of Yanchang Formation Shale Reservoirs in the Southern Ordos Basin

Zhendong Gao,¹ Yongdong Wang,¹ Xiaoyu Gu,² Hanlie Cheng ,³ and Nnamdi Puppe ⁴

¹Yanchang Oilfield Co., Ltd., Yan'an, Shaanxi 716000, China

²Laboratory of Advanced Stimulation Technology for Oil & Gas Reservoirs, Xi'an Shiyou University, Xi'an, Shanxi 710065, China

³School of Energy Resource, China University of Geosciences (Beijing), Beijing 434000, China

⁴The King's School, BP1560, Bujumbura, Burundi

Correspondence should be addressed to Nnamdi Puppe; nnamdi@ksu.edu.bi

Received 1 December 2022; Revised 26 December 2022; Accepted 31 March 2023; Published 28 April 2023

Academic Editor: Kouqi Liu

Copyright © 2023 Zhendong Gao et al. This is an open access article distributed under the Creative Commons Attribution License, which permits unrestricted use, distribution, and reproduction in any medium, provided the original work is properly cited.

Ordos Basin is a multicycle superimposed cratonic basin in northern China with a simple internal structure and a gentle stratigraphic slope. It is characterized by extensive development, numerous oil and gas-bearing layers, and complete source-reservoir-caprock assemblages. However, the research on continental shale reservoirs and gas-bearing characteristics in the southern part of the basin is not in-depth enough, which restricts the further exploration and development of shale gas in this area. In this paper, the development characteristics of pores and fractures in shale reservoirs and the gas-bearing characteristics of Yanchang Formation shale in the study area are summarized by the comprehensive use of field outcrop, core, and logging, combined with common thin section observation, scanning electron microscope observation, X-ray diffraction analysis, and other methods and techniques. Research indicates that the cement content of the sandstone in the Yanchang Formation reservoir in the south of Ordos is generally 5%-25%. The reservoir also has a large number of primary pores, secondary pores, and microfractures. The gas content of the Yanchang Formation shale represented by Chang 7 is related to both organic matter and pore structure.

1. Introduction

The so-called low permeability reservoir not only refers to its low permeability but also refers to its unique micropore structure. Its pore-throat structure is more dense than the conventional reservoir. At present, the development and exploitation of most oilfields have entered the middle and late stages, and most of them are low- and ultralow permeability reservoirs, which are difficult to develop and different from conventional reservoirs. Low-permeability oil and gas resources are widely distributed around the world, such as in the Permian Basin in the United States and the Bestling, Surgut, Ruskin, and other oil fields in the Siberia region of Russia [1, 2]. With the investment in the exploration and development of low-permeability oil and gas fields, the cumulative proven reserves of low-permeability oil and gas resources in China account for nearly half of the national

oil reserves [3]. Among them, most of the Yanchang Formation in the Ordos Basin is typically low, ultrapermeable, or tight reservoirs, and about 73.7% of the proven oil reserves are distributed in such reservoirs [4].

There are some differences in the discussion of classification and evaluation criteria among scholars from different countries, but basically, the permeability value is used as the criteria for classification of low-permeability reservoirs [5–7]. A reservoir with a permeability of 1 to 10 md is considered as low-permeability reservoir. The reservoir with permeability between 0.1 and 1 md is considered as ultralow-permeability reservoir. Permeability lower than 1 md is considered as tight reservoir. The tight sandstone of the Mesozoic Yanchang Formation in Ordos Basin and the tight sandstone and tight limestone of the Middle Sichuan Jurassic System are the most typical. They are comparable with Bakken tight oil and Eagle Ford tight oil in terms of source

rock, reservoir, formation pressure, crude oil quality, etc. Especially in source reservoir configuration, the tight oil of the Yanchang Formation in the Ordos Basin is even better than Bakken tight oil.

The research focus of low-permeability reservoirs is their microscopic pore structure characteristics. The pore structure of rocks refers to the geometric shape, size, distribution, and interconnection of pores and throats. Therefore, studying the pore-throat characteristics of reservoir rocks alone can help analyze the reservoir more accurately. The size and distribution of pore throats and various forms of their combinations are the controlling factors that affect the reservoir and reservoir percolation properties [8, 9]. Some mature technologies, such as nuclear magnetic resonance, CT scanning, X-ray diffraction, the real sandstone microscopic displacement model, and constant-rate mercury intrusion, have been used to describe the pore microstructure from different angles. In addition, a large number of scholars have studied the pore evolution, physical property changes, and diagenesis of low-permeability-ultralow permeability reservoirs (especially the Ordos Basin) through burial history analysis, tight history restoration, quantitative analysis of porosity evolution, and other methods [10–12]. The research has changed the characteristics of diagenetic evolution from qualitative evaluation to quantitative representation and established favorable reservoir facies belt evaluation indicators, ultralow permeability relatively high-quality reservoirs and “sweet spot” screening comprehensive evaluation methods in the corresponding study area [13].

The Ordos Basin is characterized by “South Oil and North Gas.” The southern part of the basin is the main production area of oil, and the upper Triassic Yanchang Formation reservoir is its main oil-producing layer [14]. However, the Triassic Yanchang Formation oil layer has the characteristics of low and ultralow permeability. The concealment and low production of oil and gas reservoirs increase the difficulty of oil and gas exploration. This paper studies the petrology, pore structure, diagenesis type, and influencing factors of shale reservoir physical properties of a certain area in the southern Ordos Basin by means of drilling and coring, cutting testing, thin section identification, mercury intrusion analysis, and cathodoluminescence observation to provide a theoretical basis for reservoir characterization and gas-bearing evaluation understanding and oil and gas exploration [15–17].

The innovation of this paper is to quantitatively analyze the gas-bearing characteristics of Chang 7 shale in Yanchang Formation, the study area, by using gas logging, on-site analysis, and isothermal adsorption experiments, and to study the shale gas content and its main control factors in different occurrence states.

2. Geological Background

The Ordos Basin is a sedimentary basin with the longest evolution time and the earliest formation history. The basin contains abundant mineral resources such as coal, salt, oil, and conventional and unconventional natural gas. There are widely developed fault zones around the basin, which

are the structural transition zone between the basin and external structural units [18, 19]. The Shajingzi fault zone is connected with the Liupanshan and Yinchuan Basins, and the southern margin of the Hetao Basin is connected to Shaanxi Province in the north and Shanxi Province in the east.

The Ordos Basin was affected by two tectonic movements at the same time, namely, the Tethys Himalayan and Pacific tectonic patterns, forming the platform basement in the Archean and early Proterozoic periods. The development and evolution of the Yanchang Formation objectively recorded the history of the occurrence, development, and extinction of this large freshwater lake basin. The Ordos Basin began to develop in the Chang 10 period, and a series of ring-shaped delta skirts were formed around the center of the lake basin, which quickly sank in the Chang 9 period, and the delta system in the Chang 10 period was completely submerged underwater [20]. By the Chang 8 period, the scale and water depth of the lake basin have increased. When the lake basin in the Chang 7 period developed to its heyday, a large area was submerged by lake water, and the area of the deep lake area also expanded rapidly. In the Chang 6 period, the decline rate of the lake basin slowed down, and the sedimentation was greatly strengthened. Two sedimentary systems developed in the northeast and southwest of the basin, forming a huge delta sedimentary body. Then, the basin sank, and the Chang 4+5 lake basin experienced another brief expansion period. Then, with the reuplift of the crust, the lake basin once again entered a shrinking period; that is, in the Chang 3 and Chang 2 periods, the lake basin was further reduced, and the delta was further swamped. At the end of Chang 1, the lake basin was uplifted to expose the surface, and the whole area became plain and swampy, which ended the deposition process of the Yanchang Formation. The sediments are generally thick in the west and thin in the east, thick in the south and thin in the north.

3. Results and Discussion

3.1. Characteristics of Reservoir Bodies. The reservoirs of the Upper Triassic Yanchang Formation in the southern Ordos Basin are mainly lacustrine delta deposits, of which Chang 2, Chang 3, Chang 6, Chang 8, and Chang 4+5 are the main oil reservoirs. Triassic oilfields mainly include Ansai Oilfield, Majiatan Oilfield, Jing’an Oilfield, Huachi Oilfield, Yanchang Oilfield, Nanliang Oilfield, and Xifeng Oilfield. The Ansai, Zhidan, and Wuqi deltas in the east of the Triassic Yanchang series have the highest degree of exploration. The exploration practice shows that the delta front near the ancient lake shoreline is the main place where large oil fields are distributed. This is because the delta sand body extends directly into the lacustrine source rock, forming a good transport layer; the delta front is developed with estuarine bars, distributary channel sands, and “blobs” and has good reservoirs. In addition, multiple sets of good reservoir cap assemblages have been formed near the shoreline due to the overlapping advance and retreat of lake water. Therefore, it is very beneficial to the formation of oil and gas reservoirs. The delta front facies sand bodies have been widely

distributed and developed for a long time. It is mainly composed of medium-fine-grained feldspar sandstone, with a single layer of 15-20 m, and its physical properties are inferior to those of distributary channel sand bodies, but it still has a certain storage capacity compared with ultralow permeability reservoirs. The Chang 8, Chang 6, Chang 4+5, Chang 3, and Chang 2 reservoirs in the study area of this paper are all sand bodies dominated by underwater distributary channels in the delta front. The delta front facies sand bodies include mouth bars, underwater distributary channels, and the sand bodies superimposed by the two.

The estuary dam is located at the estuary of the branch channel, and the sedimentation rate is the fastest. It is composed of fine and silty sand with good sorting properties. Thin fine sandstone with thick mudstone is distributed at the lower part, and thick fine sandstone with thin mudstone is distributed upward, showing a typical reverse rhythm structure vertically, reflecting the transformation of hydrodynamic conditions from low energy to high energy. Small troughed cross-bedding and deformation structures are common in sandstones, with water ripple marks visible and few biological fossils. The sand body of the estuary bar has an obvious antigrain structure, a flat bottom and convex top, and multiphase superposition. Each grain sequence cycle ends with the mudstone at the bottom turning upwards into argillaceous siltstone, siltstone, silt-fine sandstone, and fine sandstone. The thickness of a single layer of sandstone is generally 3-4 m, and the mudstone is often separated by 1-2 m. The sandstone foreset has well-developed bedding, uniform grain size, and generally high porosity and permeability, making it the best reservoir rock in the delta system. Generally, it occurs when the end of the underwater distributary river in the delta front extends into the shallow lake, and it is distributed in florets. The underwater distributary channel sand body is the underwater extension of the distributary channel of the delta plain. The shape of the sand body is similar to that of the water distributary channel sand body. The top is flat, and the bottom is convex. However, the particle size is finer than that of distributary channels. Affected by lake waves, sand bodies are widely distributed in layers with good connectivity. The composite sand body is longitudinal, the lower part is the estuary sand bar, and the upper part is the composite sand body cut and superimposed by the underwater distributary channel sand bar.

The Yanchang Formation sand body has medium structural maturity and low compositional maturity. The Chang 7 Formation is composed of black shale, dark mudstone, fine sandstone, siltstone, and tuff. The Chang 8 reservoir sandstone is dominated by fine-grained and medium-grained lithic feldspar sandstone. The Chang 6 sandstone is dominated by fine-grained lithic feldspar sandstone and feldspar sandstone. The Chang 4+5 sandstone is dominated by fine-grained lithic sandstone. The Chang 3 reservoir sandstone is dominated by fine-grained lithic feldspar sandstone and feldspar sandstone. The Chang 2 sandstone is dominated by fine-grained and medium-grained feldspar sandstone. The mica content of Yanchang Formation sandstone cuttings is very high. Extrusive rock, quartz sandstone, argillite, chert, phyllite, metamorphic quartzite, and schist are com-

mon, in addition to a small amount of chlorite cuttings, dolomite cuttings, and tuff. The cement content of the upper Triassic Yanchang Formation reservoir sandstone in the Ordos Basin is generally 5%-25%, mainly calcite, iron calcite, authigenic chlorite, kaolinite, illite, turbidite, dolomite, iron dolomite, Silica, etc. Turbidite, as the most characteristic cement in the Ordos Basin, is very unevenly distributed in the Yanchang Formation reservoir sandstone, with local distribution on the plane and discontinuous distribution on the vertical facies.

3.2. Pore Structure. The shale reservoir is very dense and has the characteristics of small particle size, complex mineral composition and structure, and strong heterogeneity. The reservoir space of the shale reservoir can not only store fluid but also provide space for fluid seepage. It can be mainly divided into two categories: pore and fracture.

In a broad sense, porosity refers to the space in the rock that is not filled by solid materials, including macroscopic cracks and microscopic pores. Microporosity refers to the interspace between rock particles, in particles (grains), and in fillings. Primary pores include primary intergranular pores and interstitial micropores. We can better identify the primary intergranular pores that have not been significantly changed by diagenesis. For example, when the intergranular pores are lined with chlorite membranes, we can basically think that the intergranular pores are the primary cause. However, in most cases, it is difficult for us to distinguish between the primary and secondary components in the intergranular pores. Therefore, in fact, the intergranular pores include primary and secondary pores, but the primary ones are the main ones.

Intergranular pores refer to the pores formed after primary intergranular pores are partially filled and transformed by interstitials during the burial and diagenesis of sandy sediments, mainly residual intergranular pores, which are generally classified as "primary pores." Such pores are generally larger in size and have good pore connectivity. This type of pore dominates the reservoirs in the study area, and residual intergranular pores are developed in each target interval. From the thin slice, the unfilled intergranular pores are mostly polygonal, with the most triangles, and the pore edges are neat and straight. A scanning electron microscope shows that ferric calcite and ferric dolomite are scattered in the pores, metasomatic debris can be seen, and the edges of some residual intergranular pores are wrapped by the early chlorite shell, which effectively prevents the secondary growth of particles. The intergranular pore size is larger, and the connectivity is good, which is the main contributing pore. In addition, it is found that the residual intergranular pores after the secondary increase of quartz are small in pore size and poor in connectivity. The micropores in the interstitial material refer to the micropores in the argillaceous matrix deposited at the same time as the sandy debris in the sandstone and the intercrystalline micropores of the sandstone authigenic minerals. It is the micropores between the authigenic clays and carbonate wafers that fill and replace the feldspar between the particles. The micropores in the interstitial material are extremely small, generally

smaller than those that can only be seen under the scanning electron microscope, which is commonly found in authigenic clays and carbonate cements. Most of these pores disappear after compaction, and only a part of them are distributed in fine sandstone with high argillaceous content. Most of the authigenic quartz and kaolinite intercrystalline micropores can be seen in the study area. Pores are small in size, uneven in distribution, and poor in connectivity.

The shale secondary pores in this area are dominated by dissolution-type secondary pores. The distribution of such pores is very limited, and the pore size is relatively small. They have a certain contribution to the pore performance of shale reservoirs. The study area has dissolved secondary pores. Through the observation and analysis of cast thin sections and a scanning electron microscope, the pores in the dissolved grains are mostly found in the feldspar grains, and the pores in the dissolved candle grains are often connected with the pores between the dissolved candle grains.

In the Triassic Yanchang Formation of the Ordos Basin, fractures are well-developed. No matter whether in outcrops around the basin or in core logging in the hinterland of the basin, natural fractures are found. Fractures are important seepage channels and effective reservoir spaces for oil and gas in low-permeability reservoirs in the Ordos Basin. Fractures are common in shale cores and thin slices. In shale reservoirs, microfractures formed due to in situ stress are small flakes with curved fracture surfaces. The crack width is generally parallel to the direction of the minimum in situ stress. In the study area, the width of such fractures is between less than a micron and tens of microns, and the fractures account for a small proportion of the total porosity of the rock. Another feature is that when the in situ stress changes significantly, the fracture changes. If the in situ stress increases along the vertical direction of the fracture, the fracture closes, resulting in a sharp drop in the formation permeability.

3.3. Evaluation of Gas-Bearing Properties. Shale gas occurs in a variety of forms. Most shale gas exists on the surface of particles and organic matter in the form of an adsorbed phase or in pores and fractures in the form of a free phase. In addition, a small amount of shale gas exists in fluids in the form of a dissolved phase. The occurrence state of shale gas in various shale gas reservoirs at home and abroad is different. Curtis [21] pointed out that the adsorbed shale gas accounts for 20%~85% of the total shale gas in five sets of shale gas reservoirs in North America. Barton et al. [22] studied the Antrim shale in the Michigan Basin and believed that the shale in this area was mainly in the adsorbed state, and the free shale gas accounted for 25%~30% of the total shale gas. Guo et al. [23] believed that the shale gas of the Yanchang Formation in the south of the Ordos Basin exists in three states: adsorbed state, free state, and dissolved state.

This section takes the Chang 7 section as the research object to further analyze the gas-bearing properties of the Yanchang Formation. According to the field analysis and test results of 74 Yanchang Formations in 8 wells, the total gas content of Chang 7 shale in each well was finally obtained. Similar to the qualitative evaluation results of

gas-bearing characteristics based on the total hydrocarbon value, the total gas content obtained by the on-site analytical method generally also has a decreasing trend from west to east and from south to north. Among them, the total gas content of the wells in the southwest is relatively high, with an average of $4.35 \text{ m}^3/\text{t}$, the total gas content of the wells in the east is slightly reduced, with an average of $2.98 \text{ m}^3/\text{t}$, and the total gas content of the wells in the south is relatively low, with an average of $2.14 \text{ m}^3/\text{t}$.

The adsorbed gas is natural gas in the adsorption state. Kerogen, clay minerals, and matrix pores can provide places for adsorption gas accumulation. Because the adsorbed gas usually contributes a lot to the total gas content, research on the adsorption capacity is of great significance for judging the gas-bearing characteristics. Isothermal adsorption experiments are one of the basic methods to study shale adsorption capacity and reservoir space characteristics. This experiment can obtain the maximum adsorbed gas content of shale.

Based on the Langmuir volume and the Langmuir pressure obtained from isothermal adsorption experiments, the adsorbed gas content of multiple samples in the Chang 7 section under the formation temperature and pressure conditions is calculated using the Langmuir formula. Research shows that the Langmuir volume of Chang 7 shale samples from the Yanchang Formation in the study area is relatively large, with an average of $4.55 \text{ m}^3/\text{t}$. The Langmuir pressure is relatively low, with an average of 2.53 MPa, and the adsorption capacity is large, with an average of $2.87 \text{ m}^3/\text{t}$ (Figures 1–3). The above characteristics indicate that the Chang 7 shale in the Yanchang Formation in the study area has a strong adsorption capacity.

Previous studies have shown that the adsorption capacity of shale for methane and other gases is roughly positively correlated with the total organic carbon content. The organic carbon content is one of the important factors affecting the adsorption capacity of shale. By analyzing the correlation between the maximum methane adsorption capacity (pumping advance), total organic carbon content, and kerogen content of the Chang 7 shale samples in the Yanchang Formation in the study area, the results show that the methane adsorption capacity is significantly related to the total organic carbon content and kerogen content. A good positive correlation (Figures 4 and 5) shows that the adsorption capacity of Chang 7 shale in the Yanchang Formation in the study area generally increases with the increase in organic matter content.

The thermal evolution stage of organic matter has an important impact on the occurrence mode and gas-bearing characteristics of shale gas. On the one hand, the more mature the organic matter, the greater the total hydrocarbon generation; on the other hand, after the organic matter generates hydrocarbons, the volume shrinkage will generate micropores, which is beneficial to the preservation of shale gas. Through the correlation analysis of the maximum methane adsorption capacity (pumping advance), the maximum pyrolysis temperature, and the hydrogen index of the Chang 7 shale samples in the Yanchang Formation in the study area (Figures 6 and 7), the results show that with the increase in

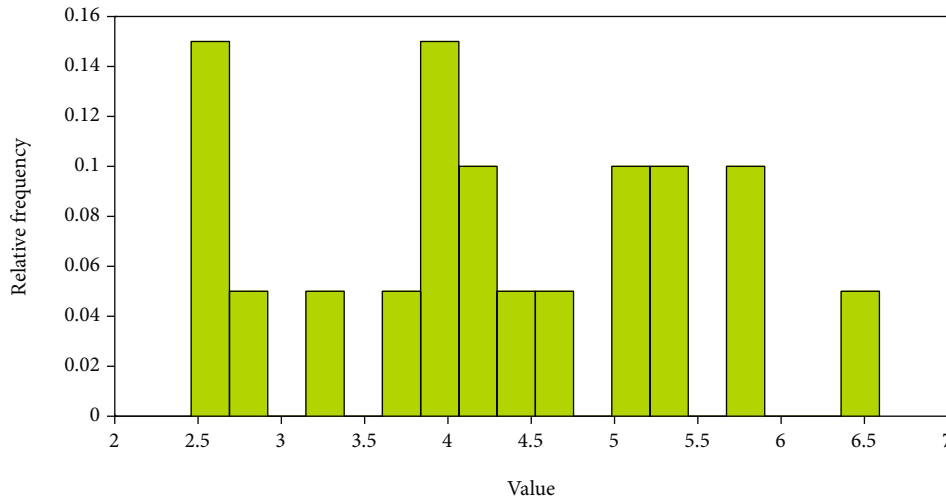


FIGURE 1: Langmuir volume histogram.

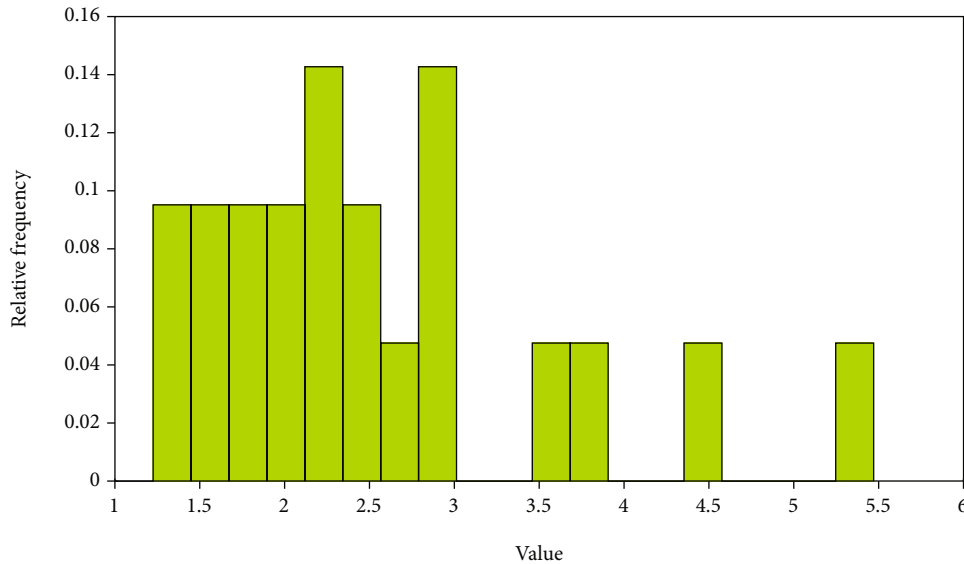


FIGURE 2: Langmuir pressure histogram.

temperature and the decrease in hydrogen index, the maximum amount of adsorbed gas in the shale also increases. It shows that the improvement of shale organic matter maturity is beneficial to the adsorption of shale gas.

Through the correlation analysis between the maximum methane adsorption amount of shale samples (the organic matter extraction advance) and the content of clay minerals, the results show that there is a certain positive correlation between the two, and the correlation is relatively poor, indicating that the adsorption of clay minerals to shale gas content has a certain effect. Micropores, especially those smaller than 50 nm, are the main determinant of the surface area of clay, which is closely related to the gas adsorption capacity of clay minerals. The clay minerals in the Chang 7 shale of the Yanchang Formation in the study area are mainly illite-mixed layers, followed by illite, with relatively low contents of chlorite and kaolinite. The results show that the maxi-

imum adsorption capacity has a positive correlation with the content of the illite/smectite mixed layer in general, while the correlation with the content of illite is not obvious, indicating that the adsorption capacity of the Chang 7 shale clay minerals in the Yanchang Formation in the study area is mainly related to the development degree of the illite/smectite mixed layer (Figure 8).

In order to study the relationship between pores and pore structure and the adsorption capacity of shale, the maximum methane adsorption capacity (pumping advance) of Chang 7 shale samples in the Yanchang Formation was analyzed for the correlation between the specific surface of meso-macropores and the specific surface of micropores. It shows that there is no obvious correlation between the maximum adsorption capacity and the specific surface of medium macropores but has a good positive correlation with the specific surface of micropores (Figure 9). That is,

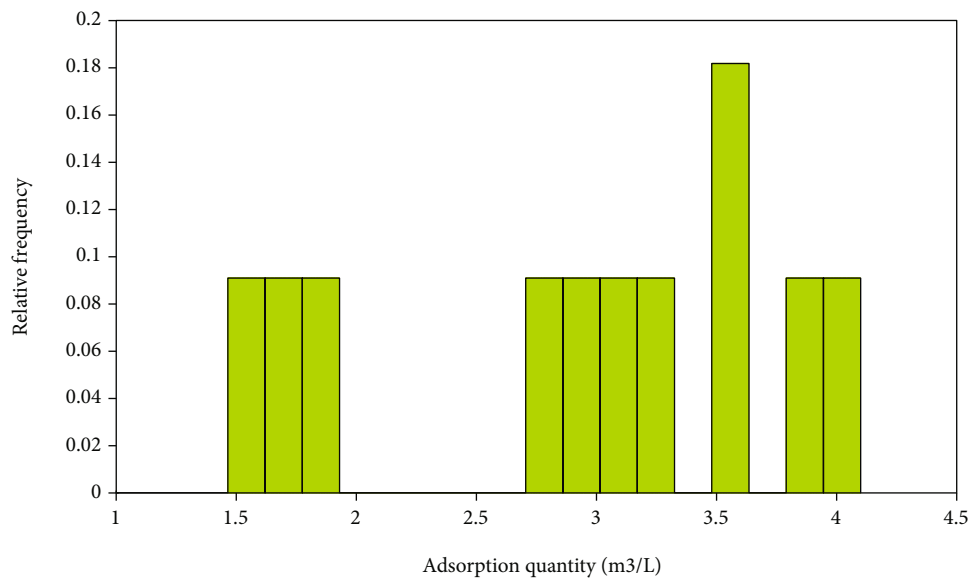


FIGURE 3: Adsorption volume histogram.

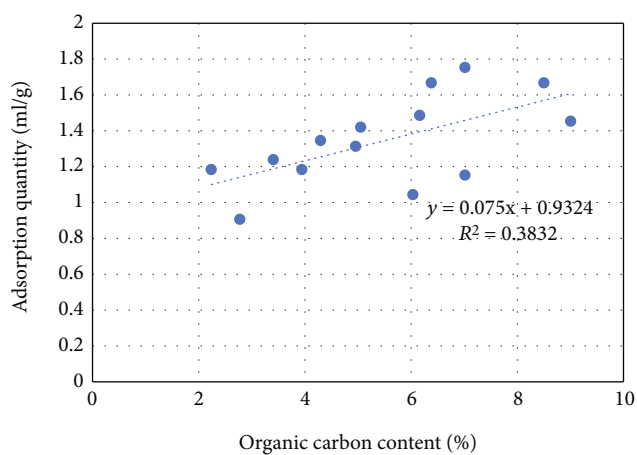


FIGURE 4: Relationship between the maximum amount of methane adsorbed and the total organic carbon content of the Chang 7 shale sample in the Yanchang Formation.

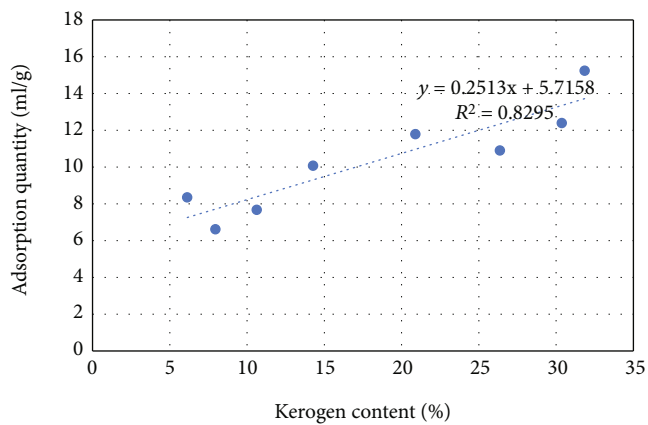


FIGURE 5: Relationship between maximum methane adsorption and kerogen content in the Yanchang Formation Chang 7 shale sample.

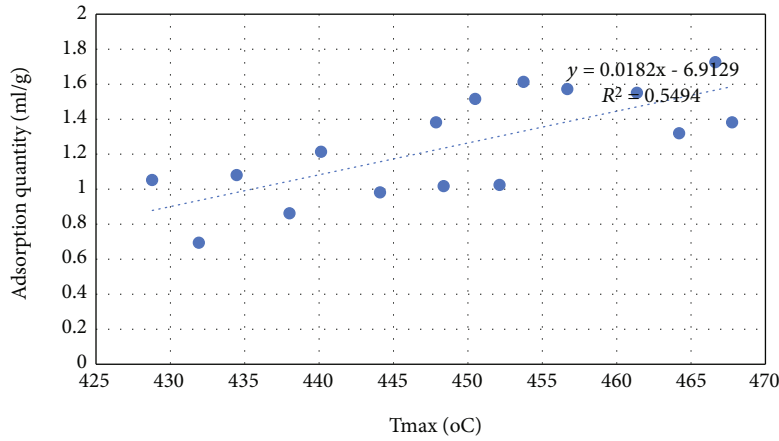


FIGURE 6: Relationship between maximum adsorption capacity and T_{max} of Chang 7 shale sample in the Yanchang Formation.

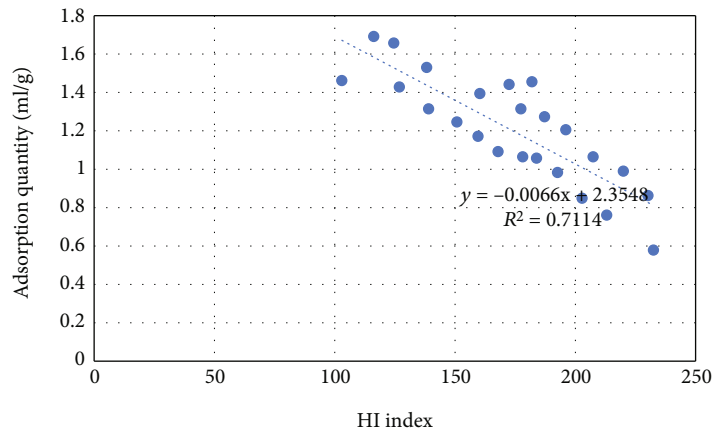


FIGURE 7: Relationship between maximum adsorption capacity and hydrogen content index of Chang 7 shale sample in the Yanchang Formation.

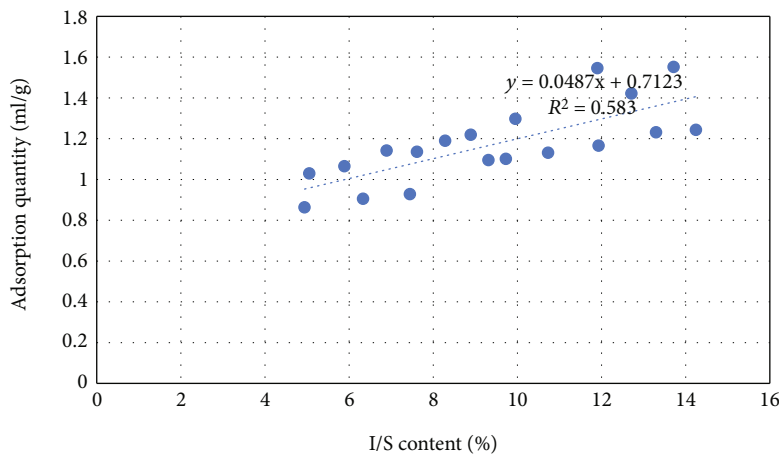


FIGURE 8: Relationship between the maximum adsorption capacity and the content of I/S mixed layers in Chang 7 shale samples.

the development of micropores in Chang 7 shale in the Yanchang Formation in the district has a certain contribution to the content of adsorbed gas in shale.

In essence, the main factors affecting the gas content of adsorbed gas in the above aspects are directly or indirectly related to the development of micropores; the direct

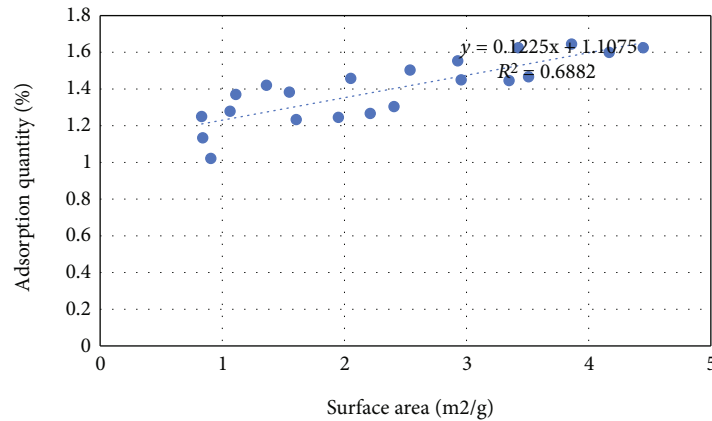


FIGURE 9: Relationship between the maximum adsorption capacity and the micropore-specific surface of the Chang 7 shale sample in the Yanchang Formation.

correlation is shown in that the specific surface area of micropores is positively correlated with the content of adsorbed gas, but not with the surface area of medium to large pore ratios. The indirect correlation is mainly related to the location of micropores, and some micropores are mainly developed in the pore space between and within organic matter. The development of micropores in the other part is mainly related to clay minerals. The reason is that the adsorption gas in shale reservoir is mainly physical adsorption, mainly caused by the van der Waals molecular force. The above characteristics determine that micropores are the most favorable places for adsorption gas enrichment.

4. Conclusion

This paper comprehensively uses the field outcrop, core, and logging data, combined with common thin section observation, a scanning electron microscope observation, X-ray diffraction analysis, and other methods and techniques, summarizes the characteristics of shale reservoir pores and fractures, and makes a quantitative analysis of the gas-bearing characteristics of the shale of the Yanchang Formation in the south of Ordos. The conclusions are as follows:

- (1) Yanchang Formation reservoirs have medium structural maturity and low compositional maturity. The cement content of the upper Triassic Yanchang Formation reservoir sandstone in the Ordos Basin is generally 5%-25%, mainly calcite, iron calcite, authigenic chlorite, kaolinite, illite, turbidite, dolomite, iron dolomite, silica, etc.
- (2) The pores are mostly authigenic quartz and kaolinite intercrystalline micropores. Pores are small in size, uneven in distribution, and poor in connectivity. The study area is dominated by the dissolution secondary pores
- (3) The Chang 7 shale in the Yanchang Formation in the study area has a strong adsorption capacity. With the increase in the maximum pyrolysis temperature of the shale and the decrease in the hydrogen index,

the maximum adsorption capacity of the shale also increases. The maximum adsorption capacity in the study area is positively correlated with the content of the illite/smectite mixed layer, but the correlation with the content of illite is not obvious. There is no obvious correlation between the maximum adsorption capacity and the specific surface of meso-macropores, but it has a good positive correlation with the specific surface of micropores

Data Availability

The figures used to support the findings of this study are included in the article.

Conflicts of Interest

The authors declare that they have no conflicts of interest.

Acknowledgments

The authors would like to show sincere thanks to those techniques who have contributed to this research.

References

- [1] M. Li, X. Pang, L. Xiong et al., "Application of mathematical statistics to shale gas-bearing property evaluation and main controlling factor analysis," *Scientific Reports*, vol. 12, no. 1, p. 9859, 2022.
- [2] D. Xiao, S. Lu, M. Shao, N. Zhou, R. Zhao, and Y. Peng, "Comparison of marine and continental shale gas reservoirs and their gas-bearing properties in China: the examples of the Longmaxi and Shahezi shales," *Energy & Fuels*, vol. 35, no. 5, pp. 4029–4043, 2021.
- [3] W. Jianfa, Z. Shengxian, F. Cunhui et al., "Fracture characteristics of the Longmaxi Formation shale and its relationship with gas-bearing properties in Changning area, southern Sichuan," *Acta Petrolei Sinica*, vol. 42, no. 4, p. 428, 2021.
- [4] K. Wang, F. Du, X. Zhang, L. Wang, and C. Xin, "Mechanical properties and permeability evolution in gas-bearing coal-

- rock combination body under triaxial conditions,” *Environmental Earth Sciences*, vol. 76, no. 24, 2017.
- [5] A. L. Anderson and L. D. Hampton, “Acoustics of gas-bearing sediments. II. Measurements and models,” *America*, vol. 67, no. 6, pp. 1890–1903, 1980.
- [6] T. Xuan, Z. H. A. N. G. Jin-Chuan, D. I. N. G. Wen-Long et al., “The reservoir property of the upper Paleozoic marine continental transitional shale and its gas bearing capacity in the southeastern Ordos Basin,” *Earth Science Frontiers*, vol. 23, no. 2, p. 147, 2016.
- [7] S. P. Meng, J. X. Zhang, H. Liu, and S. S. Liu, “Relationship between the methane carbon isotope and gas-bearing properties of coal reservoir,” *Journal of China Coal Society*, vol. 39, no. 8, pp. 1683–1690, 2014.
- [8] H. Zhang, Z. Lun, X. Zhou, H. Wang, C. Zhao, and D. Zhang, “Role of H₂O of gas-bearing shale in its physicochemical properties and CH₄ Adsorption performance alteration due to microwave irradiation,” *Energy & Fuels*, vol. 35, no. 23, pp. 19464–19480, 2021.
- [9] Y. F. N. Z. H. Changpeng and W. B. P. K. L. Huiqing, “Characterization of microscopic pore structures in shale reservoirs,” *Acta Petrolei Sinica*, vol. 34, no. 2, p. 301, 2013.
- [10] B. Yan, Y. Wang, and J. E. Killough, “Beyond dual-porosity modeling for the simulation of complex flow mechanisms in shale reservoirs,” *Computational Geosciences*, vol. 20, no. 1, pp. 69–91, 2016.
- [11] E. Ozkan, M. Brown, R. Raghavan, and H. Kazemi, “Comparison of fractured-horizontal-well performance in tight sand and shale reservoirs,” *SPE Reservoir Evaluation & Engineering*, vol. 14, no. 2, pp. 248–259, 2011.
- [12] A. H. Kohli and M. D. Zoback, “Frictional properties of shale reservoir rocks,” *Journal of Geophysical Research - Solid Earth*, vol. 118, no. 9, pp. 5109–5125, 2013.
- [13] N. Alharthy, T. Teklu, H. Kazemi et al., “Enhanced oil recovery in liquid-rich shale reservoirs: laboratory to field,” *SPE Reservoir Evaluation & Engineering*, vol. 21, no. 1, pp. 137–159, 2018.
- [14] Y. Niu, C. Wang, E. Wang, and Z. Li, “Experimental study on the damage evolution of gas-bearing coal and its electric potential response,” *Rock Mechanics and Rock Engineering*, vol. 52, no. 11, pp. 4589–4604, 2019.
- [15] H. Cheng, Y. Dong, C. Lu, Q. Qin, and D. Cadasse, “Intelligent oil production stratified water injection technology,” *Wireless Communications and Mobile Computing*, vol. 2022, Article ID 3954446, 7 pages, 2022.
- [16] Z. K. Hou, H. L. Cheng, S. W. Sun, J. Chen, D. Q. Qi, and Z. B. Liu, “Crack propagation and hydraulic fracturing in different lithologies,” *Applied Geophysics*, vol. 16, no. 2, pp. 243–251, 2019.
- [17] J. Han, H. Cheng, Y. Shi, L. Wang, Y. Song, and W. Zhnag, “Connectivity analysis and application of fracture cave carbonate reservoir in Tazhong,” *Science Technology and Engineering*, vol. 16, no. 5, pp. 147–152, 2016.
- [18] H. Cheng, J. Wei, and Z. Cheng, “Study on sedimentary facies and reservoir characteristics of Paleogene sandstone in Yingmaili Block, Tarim Basin,” *Geofluids*, vol. 2022, Article ID 1445395, 14 pages, 2022.
- [19] H. Cheng, P. Ma, G. Dong, S. Zhang, J. Wei, and Q. Qin, “Characteristics of carboniferous volcanic reservoirs in Beisantai Oilfield, Junggar Basin,” *Mathematical Problems in Engineering*, vol. 2022, Article ID 7800630, 10 pages, 2022.
- [20] K. Peng, S. Shi, Q. Zou, Y. Zhang, and G. Tan, “Gas permeability characteristics and energy evolution laws of gas-bearing coal under multi-level stress paths,” *Natural Resources Research*, vol. 29, no. 5, pp. 3137–3158, 2020.
- [21] J. B. Curtis, “Fractured shale-gas systems,” *AAPG Bulletin*, vol. 86, no. 11, pp. 1921–1938, 2002.
- [22] J. M. Barton Jr, W. P. Barnett, E. S. Barton et al., “The geology of the area surrounding the Venetia kimberlite pipes, Limpopo Belt, South Africa: a complex interplay of nappe tectonics and granitoid magmatism,” *South African Journal of Geology*, vol. 106, no. 2-3, pp. 109–128, 2003.
- [23] H. Guo, W. Jia, Y. Lei et al., “The composition and its impact on the methane sorption of lacustrine shales from the Upper Triassic Yanchang Formation, Ordos Basin, China,” *Marine and Petroleum Geology*, vol. 57, pp. 509–520, 2014.